THE RELATIONSHIP BETWEEN InGaAs CHANNEL LAYER THICKNESS AND DEVICE PERFORMANCE IN HIGH ELECTRON MOBILITY TRANSISTORS

M. MESHKINPOUR*, M. S. GOORSKY*, D. C. STREIT**, T. BLOCK**, M. WOJTOWICZ**, K. RAMMOHAN*** AND D. H. RICH***
*University of California, Los Angeles, CA 90024
**TRW, Redondo Beach, CA 90278
***University of Southern California, Los Angeles, CA 90089

ABSTRACT

The performance of InGaAs/GaAs pseudomorphic high electron mobility transistors is anticipated to improve with increased channel thickness due to reduced effects of quantum confinement. However, greater channel thicknesses increase the probability of forming misfit dislocations which have been reported to impair device properties. We characterized the composition and thickness of the active layer in $Al_{0.25}Ga_{0.75}As$ / $In_{0.21}Ga_{0.79}As$ structures with different channel thicknesses (75 Å - 300 Å) to within ± 0.005 and ± 8 Å using high resolution x-ray techniques. We determined, using Hall and rf measurements, that the device properties of these structures improved with increasing thickness up to about 185-205 Å; degraded properties were observed for thicker channel layers. Cathodoluminescence results indicate that the mosaic spread observed in x-ray triple axis rocking curves of these device structures is due to the presence of misfit dislocations. Thus, even though misfit dislocations are present, the device structure performs best with a channel thickness of ~185 Å. These results demonstrate that one can fabricate functional devices in excess of critical thickness considerations, and that these x-ray techniques provide an effective means to evaluate structural properties prior to device processing.

INTRODUCTION

InGaAs/(Al)GaAs high electron mobility transistors (HEMTs) show improved device properties over GaAs HEMTs for two reasons: (1) the higher electron mobility in InGaAs compared to GaAs and (2) the larger conduction band discontinuity at the AlGaAs/InGaAs interface which improves electron confinement in the channel. The InGaAs/(Al)GaAs HEMTs have high transconductance and low noise values which make them desirable for high speed applications [1,2]. In addition, because of their outstanding performance at millimeter wave frequencies, these device structures may be used as sensors and emitters for applications ranging from the automobile to the communications industries.

Both the composition and thickness of the InGaAs layer affect the device properties of the HEMT structure [3,4,5]. By increasing the channel layer thickness, the quantized transition levels approach the bulk energy gap resulting in better electron confinement and therefore a higher 2DEG carrier concentration [3]. Unfortunately, another effect upon increasing the InGaAs channel thickness is that of increasing the likelihood that misfit dislocations will form at the InGaAs/GaAs interface to relieve the strain [6]. Increasing the indium content is another way of improving the electron confinement by increasing the offset in the conduction band, however in this study, we will examine the effect of the channel layer thickness.

Many reports of pseudomorphic InGaAs/GaAs HEMTs include InGaAs channel layers whose thickness exceeds the Matthews Blakeslee critical thickness [1-5,6]. Most of those studies did

Mat. Res. Soc. Symp. Proc. Vol. 340. ©1994 Materials Research Society

not actually determine if misfit dislocations existed in those structures, even though degraded device performance was attributed to such defects [3-5]. Schweizer et al. [7], however, used cathodoluminescence to show that dark line defects exist in HEMT structures with thicker channel layers, and that misfit dislocations related to these dark line defects cause the Hall mobility to decrease. However, Moll et al.[5] show that the sheet carrier concentration, N_s, is the more relevant parameter in predicting device performance, but no study to date has compared N_s, the Hall mobility, μ, and device parameters such as the cutoff frequency, f_T, with the presence of misfit dislocations in these structures. Additionally, an open question remains as to whether the performance of these device structures can be predicted using non-destructive, whole wafer characterization techniques. In this study, we characterize actual HEMT structures using high resolution x-ray diffraction techniques and cathodoluminescence to predict the trends observed in the device properties of these structures.

EXPERIMENTAL PROCEDURE

Nine HEMT devices were grown by molecular beam epitaxy [1]. Starting from the substrate, they consist of a buffer layer (1750 Å), an undoped GaAs layer (3000 Å), an $In_{0.21}Ga_{0.79}As$ channel layer (thicknesses vary from 75 to 300 Å), a layer of AlGaAs (530 Å) containing a 30 Å spacer and δ-doped Si, and finally an undoped GaAs cap (50 Å).

High resolution x-ray diffraction (HRXRD) represents a promising non-destructive technique with which to characterize the structural properties (thickness and composition) and the degree of damage in the active layer of a typical HEMT structure. Double axis HRXRD was conducted on all of the device structures using a Bede D^3 diffractometer [8]. The first axis includes three (111) Si crystal faces (in the (+,-,-) configuration) that act to collimate and monochromate the incident Cu x-ray beam. The resulting $Cu_{K\alpha 1}$ radiation diffracts from the second axis (-) which is the device wafer. The x-ray generator settings were 40 kV and 30 mA. We performed ω-2θ (004) scans on the device structures over an angular range of -7000 to 3000 arcsecs so that the InGaAs and the GaAs peaks could be studied (In a ω-2θ scan, the detector is coupled to the sample's angle so that larger angular ranges may be studied than is possible in a simple rocking curve measurement). A slit 2 mm wide was placed just before the detector to reduce the background noise.

We used a dynamical simulation program [9] to determine the composition and thickness of various layers in our structures [10]. To accurately compare the experimental results to the simulations, we have added background noise to the simulated diffraction curves to achieve the same signal to noise ratio as the experimental data.

Triple axis measurements employed a Si (111) (-, +, -, +) analyzer crystal. To generate reciprocal space maps, we measured ω-2θ scans (range of 1000 arcsecs) with ranging up to ± 300 arcsecs (10 arcsec intervals) depending on the degree of mosaic tilt in the sample. Rocking curves (ω scans) using the (004) reflection substrate peak were also measured. The slit width just before the detector for all of the triple axis measurements was 1 mm. Even though we are interested in the misfit dislocations at the InGaAs/GaAs interface, we chose to do this measurement on the GaAs substrate peak rather than the InGaAs peak for two reasons. First, the GaAs peak has a much higher signal to noise ratio which is important since the signal will be significantly reduced after diffracting from the analyzer crystal. Second, the GaAs peak includes diffraction from both the substrate and the GaAs layer just below the InGaAs layer. Thus, if misfit dislocations exist at the InGaAs/GaAs interface they will affect the GaAs x-ray peak [11].

The Hall sheet carrier concentration and mobilities were measured at 77 K and 300 K using van der Pauw contacts. Cathodoluminescence (CL) measurements were performed on some of the device structures (Ref 12 describes the setup for the CL measurements).

RESULTS AND DISCUSSION

The x-ray diffraction measurements were used to determine the layer thicknesses and indium mole fraction in the channel. (004) measurements from three representative samples [(a) 75 Å, (b) 150 Å and (c) 300 Å] (which will be referred to as samples A, B and C, respectively) are shown in Figure 1. In each case, the substrate peak is at 0 arcsec (representing the deviation from the GaAs Bragg angle) and the InGaAs layer peak is at ~ -3600 arcsecs. The apparent shift of the InGaAs layer to smaller angular splitting from the substrate peak for sample A represents an interference effect described by Fewster and Curling [13] and Wie [14]. Layer thicknesses and the indium mole fraction were determined by matching simulated scans to experimental ones. Using this method, the channel thickness can be determined to ± 8 Å and the indium mole fraction to ± 0.005 [10]. For thin channel widths, the simulated scans are an excellent match to the experimental results. The diffraction scan from sample C, however, exhibits significant diffuse scattering. This diffuse scattering was observed in a sample with a channel width as thin as 250 Å. From previous SiGe studies [15], this diffuse scattering was found to be related to the presence of misfit dislocations.

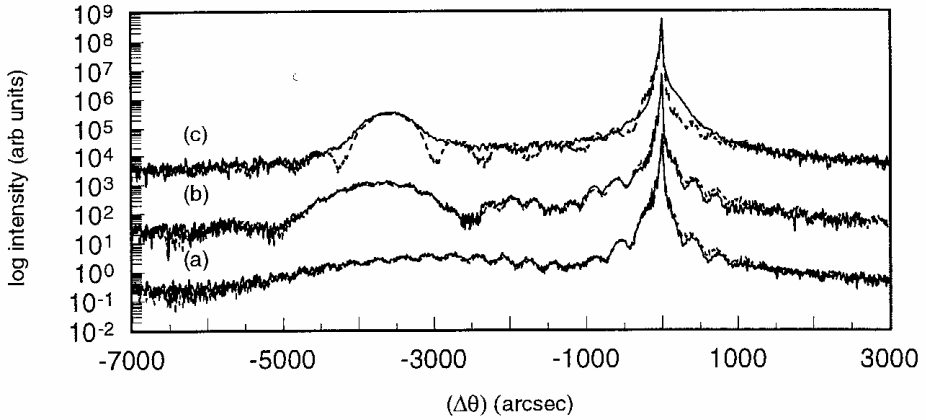

Figure 1. Best fit simulated (dashed) and experimental (solid) (004) double axis θ-2θ scans of device structures (a) A, (b) B and (c) C.

Figure 2 shows how the Hall mobility and the sheet carrier concentration vary with the InGaAs channel thickness at 300 K. The mobility is relatively constant with increasing thickness, however drops drastically for thicknesses greater than 250 Å. This result suggests that the effective critical thickness of this device structure is 250 Å. However, the sheet carrier concentration appears to be more sensitive than the mobility to damage in the device structure. The carrier concentration initially increases with channel thickness up to about 150-185 Å. At 77 K, the sheet carrier concentration drops between 185-205 Å. This trend can be attributed to the increase in carrier confinement with increasing channel width, and therefore the increase in the 2 DEG concentration. However, for thicknesses greater than 150-185 Å, the carrier concentration decreases. Preliminary rf measurements of fabricated device structures with 0.1 mm gate [16] also

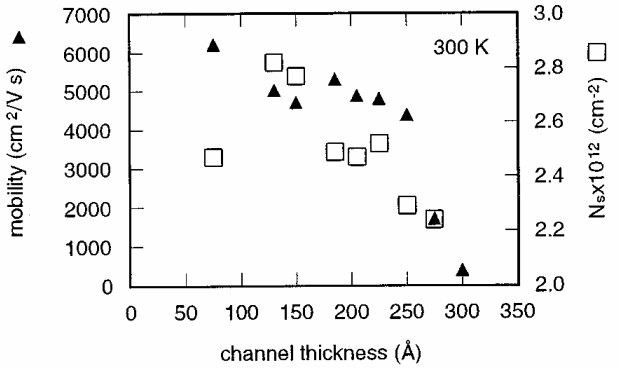

Figure 2. Variation of Hall mobility and sheet carrier concentration with channel thickness at 300 K.

show that f_T increases with channel thickness up to 185 Å, but that f_T decreases substantially for devices with thicker channels.

Even though double axis measurements provide excellent data for determining the structural properties of a device structure, triple axis measurements are more useful for determining the presence of misfit dislocations or mosaic tilt because the effect of strain and mosaic tilt on the diffraction patterns may be distinguished from each other. The data from the triple axis scans for device structures A, B and C were converted to reciprocal space maps [17] shown in figure 3 (a), (b) and (c), respectively. The center of the contours corresponds to the (004) substrate peak. The axes, q_y and q_z, represent the deviation from the Bragg reflection in reciprocal space and more importantly the degree of strain and mosaic tilt, respectively. As the channel width increases, the degree of mosaic spread (extension along q_y axis) increases (q_z represents strain). Of significance is the fact that even though device structure B has mosaic tilt, there is no indication of diffuse scattering in the double axis scan, nor any significant drop in the sheet carrier concentration or the mobility.

In an attempt to quantify our results, we calculated the area under the triple axis rocking curves. These rocking curves are equivalent to scans at q_z=0 (over a range of 400 arcsecs along q_y), and therefore are a good measure of the degree of mosaic tilt. Figure 4 shows how this cal-

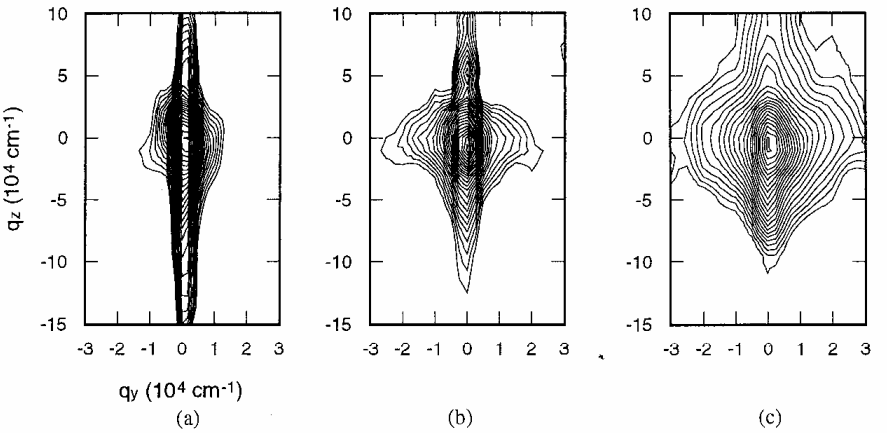

Figure 3. Reciprocal space maps of device structures (a) A, (b) B and (c) C.

culated area (average of scans along [110] and [$\bar{1}$10]) varies with the thickness of the buried layer. The area under the rocking curves increases significantly for channel thicknesses greater than 150 Å, thus implying a correlation to the trend observed with the sheet concentration. As

the area under the diffraction curve or the degree of mosaic spread increases, the sheet concentration decreases. Moll et al. [5] indicated that f_T and I_D, the drain current, were more strongly related to the sheet concentration than the mobility.

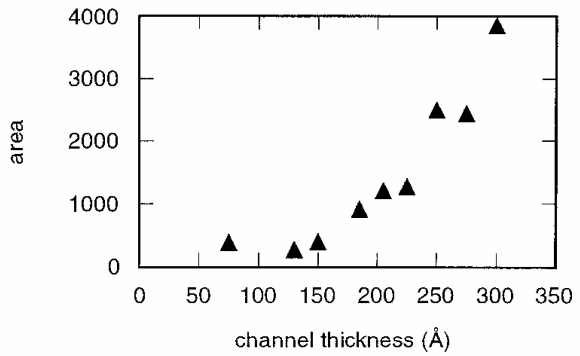

Figure 4. Variation of area under rocking curve with channel thickness.

Cathodoluminescence (CL) measurements illustrate the origin of this mosaic tilt. Figure 5 (a), (b) and (c) shows CL micrographs of device structures A, B and C, respectively. Device structure A seems to be free of misfit dislocations which would explain its high carrier concentration and electron mobility. At the other extreme, device structure C has a dense network of dislocations running along both the [110] and [$\bar{1}$10] directions. In device structure B, however, misfit dislocations seem to form primarily along the [$\bar{1}$10] [18] direction, and are apparently few in number allowing for good device performance. Based on the similarity in behavior between N_S and the area (under a rocking curve) with increasing channel thickness, triple axis diffraction techniques may be able to predict device performance before the actual device has been completed. The added advantage associated with the triple axis measurements is the fact that an entire wafer may be characterized, so that subsequent processing steps may be carried out on the same material.

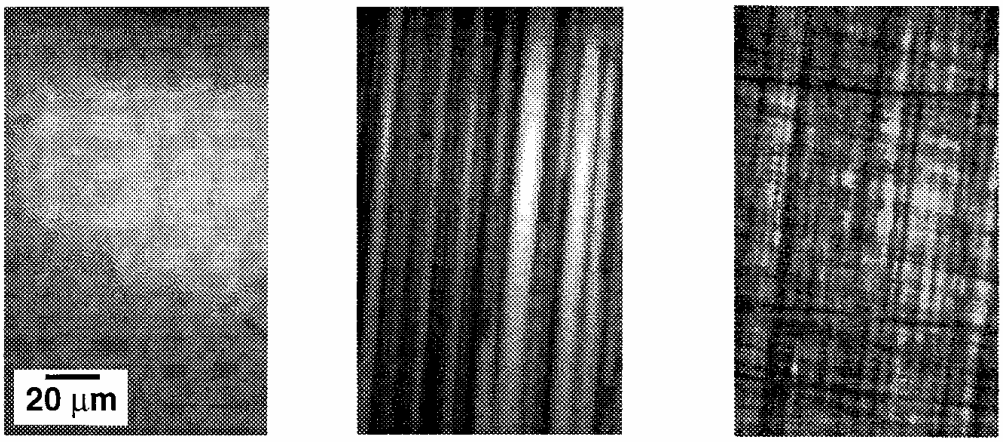

Figure 5. CL micrographs of device structures (a) A, (b) B and (c) C.

CONCLUSION

Double axis diffraction measurements allow us to determine the composition and thickness of the InGaAs layer to within ± 0.005 and ± 8 Å, respectively. Results from our CL and triple axis measurements are more sensitive to the presence of misfit dislocations and correlate well with

each other as well as with the sheet concentration. Contrary to the implications derived from the double axis and Hall mobility measurements, the effective critical thickness of these HEMT structures is not 250 Å. The presence of misfit dislocations does not necessarily impair the device performance, and in fact we see that the best device structures contain misfit dislocations. Most importantly, HRXRD techniques prove to be an excellent tool in characterizing device structures as well as possibly predicting device properties before further processing. Our future efforts on this topic will include transmission electron microscopy and a more complete set of rf measurements on these device structures.

ACKNOWLEDGMENTS

The work performed at UCLA was funded by TRW, the UC MICRO program, the National Science Foundation through grant DMR 9208766 and the National Defense Science and Engineering Graduate Fellowship program.

REFERENCES

1. D.C. Streit, K.L. Tan, R.M. Dia, J.K. Liu, A.C. Han and J.R. Velebir, IEEE Elec. Dev. Lett. **12**, 149 (1991).
2. K.L. Tan, R.M. Dia, D.C. Streit, L.K. Shaw, A.C. Han, M.D. Sholley, P.H. Liu, T.Q. Trinh, T. Lin, H.C. Yen, IEEE Elec. Dev. Lett. **12**,23 (1991).
3. L.D. Nguyen, D.C. Radulescu, M.C. Foisy, P.J. Tasker and L.F. Eastman, IEEE Trans. Elec. Dev. **36**, 833 (1989).
4. A. Fischer-Colbrie J.N. Miller, S.S. Laderman, S.J. Rosner and R. Hull, J. Vac. Sci. Technol., **B 6** 620 (1988).
5. N. Moll, M.R. Hueschen and A. Fischer-Colbrie, IEEE Trans. Elec. Dev. **35**, 878 (1988).
6. J.W. Matthews and A.E. Blakeslee, J. Crys. Growth **27**,118 (1974).
7. T. Schweizer, K. Kohler, W. Rothemund and P. Ganser, Appl. Phys. Lett. **59**, 2736 (1991).
8. Bede Scientific Instruments Ltd, Lindsey Park, Bowburn, Durham DH6 5PF, U. K.
9. RADS Rocking Curve Analysis by Dynamical Simulation, Bede Scientific Instruments Ltd., UK (1992).
10. M. Meshkinpour, MS. Goorsky, K.Matney, D.C. Streit and T. Block, J. Appl. Phys., submitted.
11. G.S. Green, B.K. Tanner, S.J. Barnett, M.T. Emery, A.D. Pitt, C.R. Whitehouse and G.F. Clark, Philos. Mag. Lett. **62,** 131 (1990).
12. D.H. Rich, K. Rammohan, Y. Tang, H.T. Lin, J. Maserjian, F.J. Grunthaner, A. Larsson and S.I. Borenstain, Appl. Phys. Lett. **64**, 1 (1994).
13. P.F. Fewster and C.J. Curling, J. Appl. Phys. **62**, 4154 (1987).
14. C.R. Wie, J. Appl. Phys. **66**, 985 (1989).
15. S.R. Stiffler, J.H. Comfort, C.L. Stanis, D.L. Harame, E. de Fresart and B.S. Meyerson, J. Appl. Phys. **70**, 1416 (1991).
16. D.C. Streit et al., to be submitted.
17. B.K. Tanner and D.K. Bowen, J. Crys. Growth **126**, 1 (1993).
18. G.P. Watson, D.G. Ast, T.J. Anderson, B. Pathangey and Y. Hayakawa, J. Appl. Phys. **71**, 3399 (1992).